

# Supplemental figures to the abstract

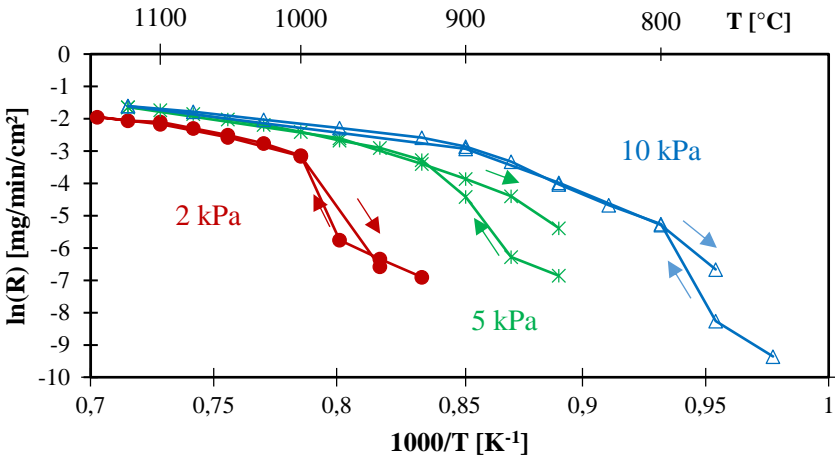


Fig. 1.a.: Arrhenius plots of the deposition rate R.  $\alpha = 13$ ,  $Q_{tot} = 150$  sccm.

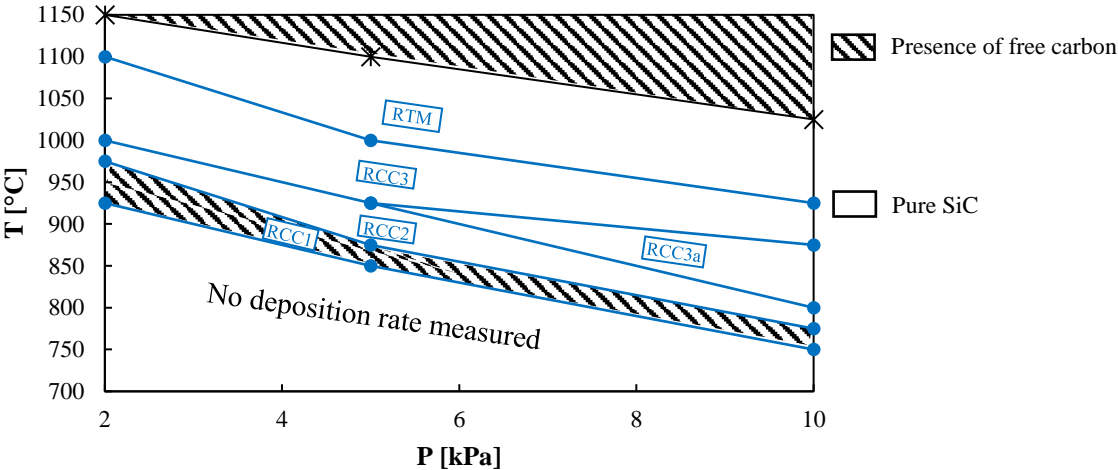


Fig. 1.b.: P-T diagram showing the different deposition regimes identified on the Arrhenius plots.  $\alpha = 13$ ,  $Q_{tot} = 150$  sccm.

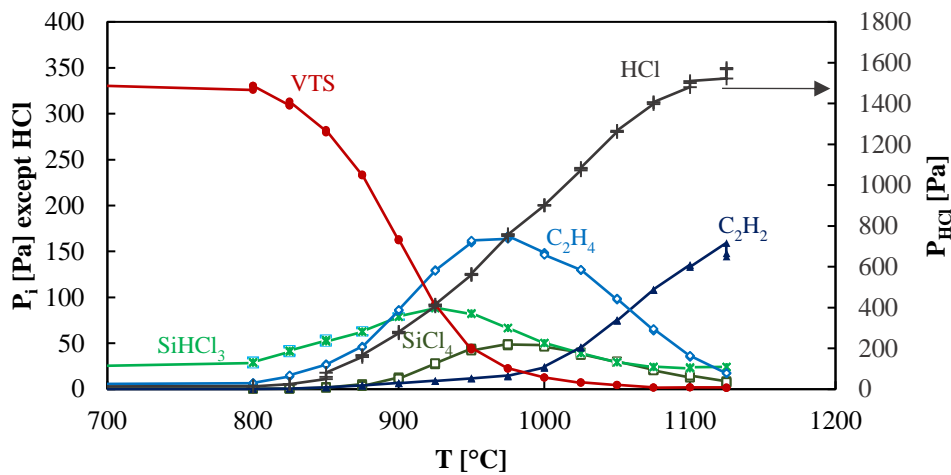


Fig. 2: Gas phase concentration, as measured by FTIR at the reactor outlet, as a function of temperature.  $P = 5 \text{ kPa}$ ,  $\alpha = 13$ ,  $Q_{\text{tot}} = 150 \text{ sccm}$ .

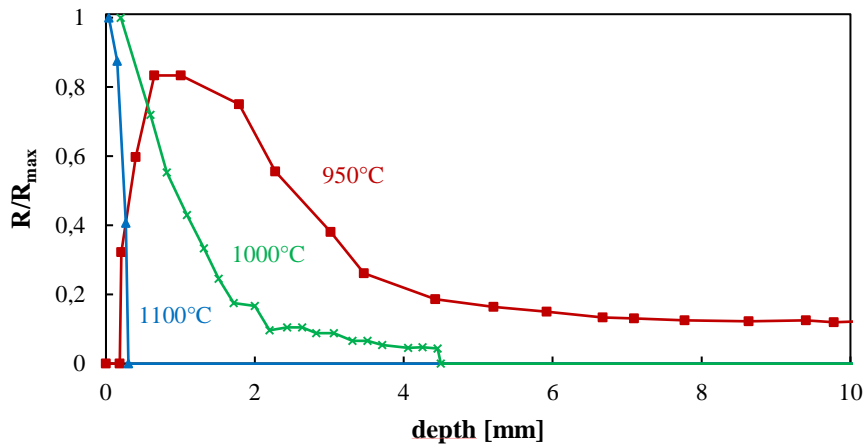


Fig. 3: Normalized deposition rate of pure SiC along the model channel pore ( $x = 0 \text{ mm}$  at the entrance of a  $100 \mu\text{m}$ -opening channel).  $P = 2 \text{ kPa}$ ,  $\alpha = 13$ ,  $Q_{\text{tot}} = 300 \text{ sccm}$ .

Position	0 mm	0,3 mm	1 mm
MEB image			
EDX analysis	C (at. %) = 97,3 Si (at. %) = 2,7	C (at. %) = 49,7 Si (at. %) = 50,3	C (at. %) = 49,3 Si (at. %) = 50,7

Fig. 4: SEM images of the porous substrates after CVI at  $T = 950^\circ\text{C}$ ,  $P = 2 \text{ kPa}$ ,  $\alpha = 13$ ,  $Q_{\text{tot}} = 300 \text{ sccm}$ , at three different positions along the model channel pore ( $x = 0 \text{ mm}$  at the entrance of the  $100 \mu\text{m}$ -opening channel).